

Urbach rule in mixed single crystals of $\text{Zn}_x\text{Cd}_{1-x}\text{Se}$

L. Samuel and Y. Brada

Racah Institute of Physics, Hebrew University, Jerusalem 91904 Israel

A. Burger and M. Roth

School of Applied Sciences, Hebrew University, Jerusalem 91904 Israel

(Received 4 August 1986; revised manuscript received 16 March 1987)

The dependence of the absorption coefficient on the photon energy and on temperature near the fundamental absorption edge was measured in mixed single crystals of $\text{Zn}_x\text{Cd}_{1-x}\text{Se}$, for $x=0, 0.04, 0.3, 0.4$, and 1 . Exponential dependence of that coefficient according to the Urbach rule was observed. The thermal dependence of the slope parameter indicates that the absorption is influenced by the phonon-induced electric microfields and not by compositional or structural potential fluctuations. Up to about 90 K the magnitude of $\hbar\omega_0$ fits the energy of the piezoelectric LA phonon, and at higher temperatures $\hbar\omega_0$ fits the energy of the LO phonon. The energy $\hbar\omega_0$ of the LO phonons varies linearly within the experimental error with x , from 27 meV for CdSe to 31 meV for ZnSe, and is in good agreement with the Raman spectra measured for these amalgamated behavior-type crystals. The energy gap, measured at room temperature, and the value of E_0 change linearly with composition for the hexagonal phase crystals. The absorption process can be considered as an internal Franz-Keldysh effect, caused by the phonon-generated electric fields. It is described in the framework of the Dow-Redfield model, which ascribes the Urbach rule to the ionization of the exciton, as an extension of the Stark shift.

INTRODUCTION

The optical-absorption coefficient near the fundamental absorption edge depends on the photon energy and temperature according to Urbach rule:^{1,2}

$$\alpha = \alpha_0 \exp[S(E - E_0)], \quad (1)$$

where α_0 and E_0 are fitting parameters which are independent of temperature. That behavior of the absorption coefficient has been observed in ionic materials as well as in covalent and doped crystals. From the application of the one-electron approximation for direct transitions, which is the case in I-VII and II-VI compounds, it would be expected that³

$$\alpha \propto (E - E_0)^{1/2} \quad (2)$$

which is not in agreement with the experimentally observed absorption spectra.

The exponential dependence of the absorption coefficient has been observed also in amorphous^{4,5} and polycrystalline materials, but while in this type of material the slope parameter S is independent of temperature, in single crystals S is temperature dependent.

Another pertinent parameter is $\sigma = SkT$, where k is the Boltzmann constant and T is the absolute temperature. In pure ionic crystals σ has been found to vary as:^{6,7}

$$\sigma = \sigma_0 \frac{2kT}{\hbar\omega_0} \tanh \left[\frac{\hbar\omega_0}{2kT} \right], \quad (3)$$

where σ_0 and $\hbar\omega_0$ are constants.

The energy $\hbar\omega_0$ of Eq. (3) has been found experimentally to fit the energies of the phonons in the crystal. In al-

kali halides⁸ $\hbar\omega_0$ fits the energy of the LO phonon over the whole temperature range. In pure single crystals of II-VI compounds, which are not only partially ionic, but also piezoelectric, the value of $\hbar\omega_0$ depends on the temperature range. Up to about 80 K $\hbar\omega_0$ fits the energy of the piezoelectric LA phonon. From that temperature up $\hbar\omega_0$ fits the energy of the LO phonon. This behavior has been shown experimentally for ZnS of various crystalline structures⁹ and presently also for CdSe and ZnSe as well.

In contrast to the pure crystals, the absorption edge of mixed crystals has not yet been extensively studied. The mixed II-VI compound crystals do, in many cases, change their optical and electronic properties continuously with composition. Thus, for example, their absorption edge can, in many cases, be adjusted to fit a specific energy range.

The mixed crystals can be divided into two classes, according to the compositional dependence of their spectral properties. In some known amalgamated-behavior-type crystals, such as $\text{Zn}_x\text{Cd}_{1-x}\text{Se}$ (Ref. 10) and $\text{Zn}_x\text{Cd}_{1-x}\text{S}$ (Ref. 11), the physical crystal properties vary continuously with composition. The average lattice constant, the phonon energies, and other properties as well, vary continuously, usually nearly linearly, with composition, i.e., with x , although anharmonic effects may appear as a consequence of the mixing of the two constituents. In persistent-behavior-type crystals, examples of which have been found in $\text{ZnS}_x\text{Se}_{1-x}$ (Ref. 12) and $\text{CdS}_x\text{Se}_{1-x}$,¹³ the two constituents exhibit two independent Raman spectra, probably due to localized LO-phonon fields associated with the pure constituents.¹⁴

The purpose of the present research is to study the optical-absorption process near the fundamental absorp-

tion edge in $\text{Zn}_x\text{Cd}_{1-x}\text{Se}$ single crystals. Through the thermal dependence of the σ parameter it can be deduced whether the compositional fluctuations or the crystal phonons have the major influence on the absorption process. The character of the thermal shift of the absorption edge can also be used to strengthen the consequent conclusions.

THEORY

There are two main theories suggested for the explanation of the Urbach rule in pure single crystals.

The more commonly used theory, developed by Toyozawa and Schreiber,¹⁵ ascribes the exponential shape of the absorption coefficient to the coexistence of free excitons and momentarily localized self-trapped excitons. In this case, the exciton after being created interacts with the surrounding phonons through their deformation potential.

The self-trapping of excitons model¹⁶ is applicable to highly ionic crystals, like the alkali halides, and to excimers in molecular crystals. The local nature of the self-trapping limits its applicability to cases in which the excitation radius is small and the excitation is localized, or equivalently the effective mass of the hole is much larger than the electron effective mass. In alkali halides, the coupling to phonons is strong, and because of the high ionicity the effective mass of the hole is about 10 times larger than that of the electron. Therefore, when the hole is trapped in a small radius state, the electron is attached to it by the strong Coulombic interaction due to the small dielectric constant.

In II-VI compounds the exciton radius is much larger than in the alkali halides, due to the higher dielectric constants which decrease the Coulombic attraction between the hole and the electron. In addition, according to data obtained by other methods, for pure crystals the ratio m_h/m_e (Ref. 17) is smaller than 10, and its value is about 5–6, or even less. Furthermore, since the trapping of the exciton is determined by the exciton-phonon coupling constant, which is quite small in II-VI compounds, the exciton there is almost free.

For all of these reasons the Dow and Redfield (DR) model gives a better description of the optical-absorption mechanism in the II-VI compound single crystals.

The main features of the theory will be presented here, and for further details see the Appendix.

According to the DR (Ref. 18) theory the phonon-induced electric microfields create new energy states in the forbidden energy gap below the ground state of the 1S exciton. These states enable the exciton to tunnel out from its quasibound state into the potential trough beyond the Coulombic potential barrier, or equivalently—to be ionized and have a part of its wave function free. This is an internal Franz-Keldysh effect caused by the phonon-generated electric microfields. It is the extension of the weak-field Stark effect beyond the mere polarization of the exciton to its full ionization.

According to theoretical calculations carried out for electroabsorption, when an external electric field (F_e) is applied on the crystal:¹⁹

$$\ln(\alpha) \propto \frac{C}{F_e} (E - E_0), \quad (4)$$

where C and E_0 are constants.

When the field is induced by internal factors, the external field F_e is replaced by an average effective field. In disordered systems, like in the amorphous and polycrystalline materials, the average field is due to random spatial potential fluctuations. Therefore the average field is temperature independent. In single crystals the electric fields are induced either by phonons or by charged impurities. When the electric fields are induced by the impurities in the crystal,^{20,21} the average field depends both on the temperature and on the concentration of those impurities. This is the case in doped covalent materials. In alkali halides the fields are induced by the LO phonons over the whole temperature range. In II-VI compounds those phonons dominate the electric fields only at the higher-temperature range. Assuming a Gaussian distribution of those fields yields:

$$\langle F^2 \rangle = \frac{\hbar\omega_0}{3\pi\epsilon^*} q_c^3 \coth \left[\frac{\hbar\omega_0}{2kT} \right], \quad (5)$$

where $\hbar\omega_0$ is the energy of the LO phonon, $(1/\epsilon_\infty - 1/\epsilon_0) = \epsilon^*$ is the effective dielectric constant, and q_c is the polaron cutoff wave vector. The best evaluation of q_c , suggested by DR and based on the uncertainty principle yields:

$$F_{\text{rms}} = \frac{2\epsilon_0\hbar\omega_0}{\sqrt{3}\epsilon^*ea\pi} \coth \left[\frac{\hbar\omega_0}{2kT} \right], \quad (6)$$

where a is the 1s exciton radius.

The value of “ a ” in the pure crystals is computed from the binding energy E_b which equals $e^2/2\epsilon_0a$.

Evaluation of the electric fields induced by the piezoelectric LA phonons is carried out with the third-rank piezoelectric tensor e :²²

$$\mathbf{F} = \frac{4\pi}{eq} \mathbf{q} \cdot \mathbf{e}(\nabla \mathbf{u}), \quad (7)$$

where $\nabla \mathbf{u}$ is the displacement vector. The influence of piezoelectric fields on the Urbach rule has also been shown for GaAs (Ref. 23) and ZnS.⁹

Comparing Eqs. (1) and (4) results in

$$S = \frac{C}{F}. \quad (8)$$

Hence, the thermal dependence of the slope parameter and consequently of the σ parameter can indicate the pertinent source of the electric microfields which influence the absorption process.

EXPERIMENTAL PROCEDURE

The $\text{Zn}_x\text{Cd}_{1-x}\text{Se}$ single crystals were grown from a high-temperature solid solution in Se,²⁴ using the temperature-gradient solution zoning (TGSZ) technique. The growth starts from purified CdSe and ZnSe powders in the desired ternary composition with the addition of 10 at. % Se. The crystalline structure of the ternary solid solution depends on their composition. For $x < 0.4$ the crystals are of hexagonal (2H) structure.¹⁰ For $x > 0.6$ the crystals are of cubic (3C) structure. For $0.4 < x < 0.6$ both

structures appear, and the bulk is polycrystalline. In the present research no single crystal could be obtained with $x=0.5$, and a polycrystalline boule grew instead.

The crystals that were measured in the present report were of compositions $x=0, 0.04, 0.3, 0.4$, and 1 . All of them, except ZnSe ($x=1$) were of hexagonal phase. ZnSe was of cubic structure.

The crystals were cut into platelets, in most samples with their c axis perpendicular to the largest surfaces. The samples were ground and etched in a Br-methanol solution to 80–150 μm thickness.

The experimental apparatus consisted of a 12-V 100-W tungsten-halide light source, a Spex 1401 double monochromator and a computerized system to run the experiment. The samples were glued to a metal disc in a Helitrans cryostat, and the measurement temperatures were between 13 and 300 K. The zero-absorption value for calibration purposes was assumed to exist at about 1000 \AA from the absorption edge. This calibration then includes also scattering and reflection corrections, since in the measured energy range those factors change only slightly, while the absorption changes by several orders of magnitude. The spectral responsivity of the measuring system was also normalized. Samples with their c axis parallel to their largest surfaces have been measured with polarized light with the electric vectors both $\mathbf{E} \perp \mathbf{c}$ and $\mathbf{E} \parallel \mathbf{c}$.

RESULTS AND DISCUSSION

All the measured samples, over the whole compositional range and at all temperatures have shown the exponential dependence of the absorption coefficient on energy as described by the Urbach rule. The slope parameter S and the σ parameter were obtained from the plot of $\ln(\alpha d)$ versus the photon energy, where d is the sample thickness.

The thermal dependence of the σ parameter in CdSe ($\mathbf{E} \perp \mathbf{c}$ polarization), ZnSe, $\text{Zn}_{0.3}\text{Cd}_{0.7}\text{Se}$ (both polarizations), and $\text{Zn}_{0.4}\text{Cd}_{0.6}\text{Se}$ (both polarizations) are shown in Figs. 1–6. Similar dependence for $\text{Zn}_{0.04}\text{Cd}_{0.96}\text{Se}$ has been observed as well.

The σ parameter increases with temperature according to Eq. (3). The values of σ_0 and $\hbar\omega_0$ for each curve have been calculated as fitting parameters. The values of σ_0 , $\hbar\omega_0$, and E_0 which appear in Eq. (3) are shown in Table I for all the measured crystals.

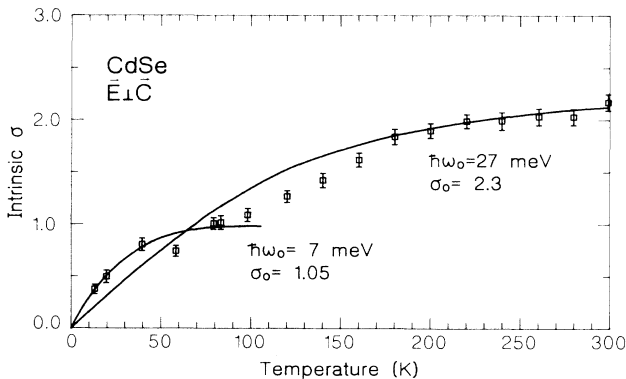


FIG. 1. Intrinsic σ vs temperature in CdSe, $\mathbf{E} \perp \mathbf{c}$ polarization.

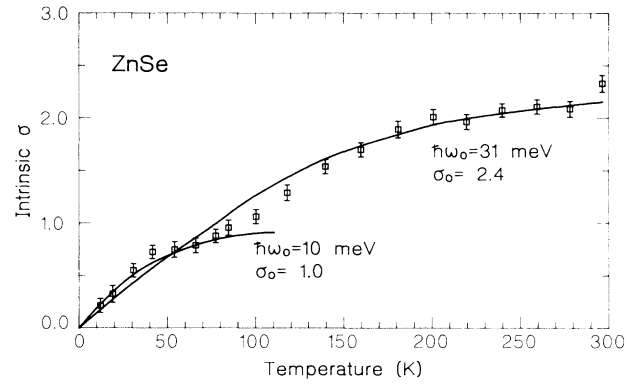


FIG. 2. Intrinsic σ vs temperature in ZnSe.

Since the measured crystals are of the amalgamated-behavior type, the values of the dielectric constants ϵ_0 and the radius of the exciton a have been considered as approximately linearly dependent on composition between the values of the pure crystals ($x=0,1$). Raman measurements show a linear dependence of the energy of the LO phonons in $\text{Zn}_x\text{Cd}_{1-x}\text{Se}$ on composition.¹⁰ The energies of the LA phonons have been calculated by the ratio of the LO and LA phonons' energies in similar II-VI crystals with the same crystalline structure.

The thermal shift of the energy gap has also been measured. The gap energy was measured at $ad=9.0$, which corresponds to $\alpha \approx 900 \text{ cm}^{-1}$. The experimentally observed dependence²⁵ of the gap energy on temperature supports the theoretical argument that the thermal shift is caused by the phonon-induced electric fields, which decrease the effective band gap by an internal Franz-Keldysh effect.

Figure 7 shows that the compositional dependence of the absorption-edge energy at room temperature is linear for all these hexagonal-phase crystals.

The thermal dependence of the σ parameter indicates that the electric microfields which are involved in the absorption process are induced by phonons and not by compositional or structural potential fluctuations. Up to about 80–90 K the value of $\hbar\omega_0$ fits the energy of the LA

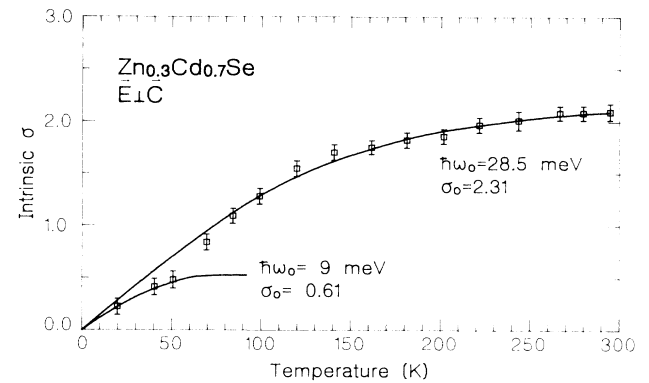


FIG. 3. Intrinsic σ vs temperature in $\text{Zn}_{0.3}\text{Cd}_{0.7}\text{Se}$, $\mathbf{E} \perp \mathbf{c}$ polarization.

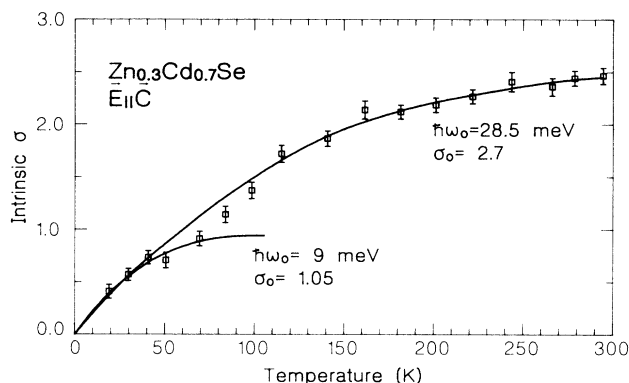


FIG. 4. Intrinsic σ vs temperature in $\text{Zn}_{0.3}\text{Cd}_{0.7}\text{Se}$, $\text{E}||\text{C}$ polarization.

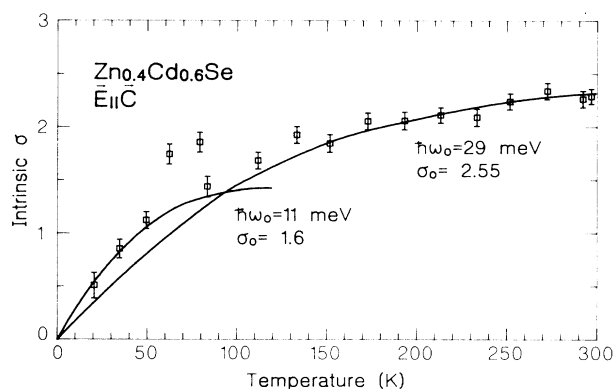


FIG. 6. Intrinsic σ vs temperature in $\text{Zn}_{0.4}\text{Cd}_{0.6}\text{Se}$, $\text{E}||\text{C}$ polarization.

phonons, and from that temperature above, $\hbar\omega_0$ fits the energy of the LO phonons. The values of σ_0 vary within the range of values known for other II-VI compounds pure single crystals.⁶

The value of σ_0 for $\text{E} \perp \text{C}$ is lower than for $\text{E} || \text{C}$. Similar phenomena have been observed for ZnS (Ref. 9) of various crystalline structures. The values of E_0 which appear in Eq. (1) have been deduced from the plots of $\ln(\alpha d)$ versus photon energies at various temperatures. E_0 for the measured crystals varies continuously with composition as shown in Fig. 7.

Extrinsic absorption by impurities has been observed at energies far below the absorption edge. The σ values of that absorption are 1–2 orders of magnitude less than those of the intrinsic absorption.

EXAFS measurements²⁶ of another amalgamated-behavior-type crystal of similar structure show that the two constituents distribute randomly over the crystal, and that the system has a well-defined crystalline structure. The cation sublattice remains almost fixed, and only the anion sublattice is somewhat distorted.

Our results show that the dominant electric microfields are determined by the single phonon frequencies of a well-ordered structure. However the compositional and structural potential fluctuations are the reason for the ap-

pearance of long-lived excitons in²⁷ delayed photoluminescence measurements. Since a large fraction of the luminescence comes from tail states, which absorb only about 1% as strongly as the bulk states,²⁸ and since these states correspond to highly disordered regions of the solid, photoluminescence spectra are far more sensitive to potential fluctuations than absorption spectra.

When structural disorder increases, it influences also the absorption spectra. Among the measured samples $\text{Zn}_{0.4}\text{Cd}_{0.6}\text{Se}$ is the closest to the range where both crystalline structures appear in the same bulk. According to the mentioned EXAFS measurements,²⁶ the nearest-neighbor distance depends on the identity of that neighbor. When the concentrations of the two constituents of the mixed crystals are close, the size of the misfits and the number of dislocations is large which results in local-scale disorder. The effects of that disorder have been observed also through anharmonic effects in second-order Raman spectra.¹⁰

The influence of the structural disorder on the character of the absorption spectra of $\text{Zn}_{0.4}\text{Cd}_{0.6}\text{Se}$ results both in the relatively large discrepancy between theory and the experimental results of the thermal dependence of the σ parameter, and also in the especially low values of σ_0 for the LO-phonon range, which are also close to the σ values of the LA-phonons range, for both polarization directions. The influence of disorder has also been observed in this case through the relatively large and well-defined σ values of the extrinsic absorption, far below the absorption edge and over the whole measured temperature range.

SUMMARY

It has been shown that in mixed single crystals of $\text{Zn}_x\text{Cd}_{1-x}\text{Se}$ the absorption coefficient near the fundamental absorption edge is energy and temperature dependent according to the Urbach rule, like in the case of pure II-VI compound single crystals. The thermal dependence of the slope parameter indicates that the electric fields which influence the absorption coefficient are the phonon-induced fields, and not those which are generated by the compositional or structural fluctuations. Up to about

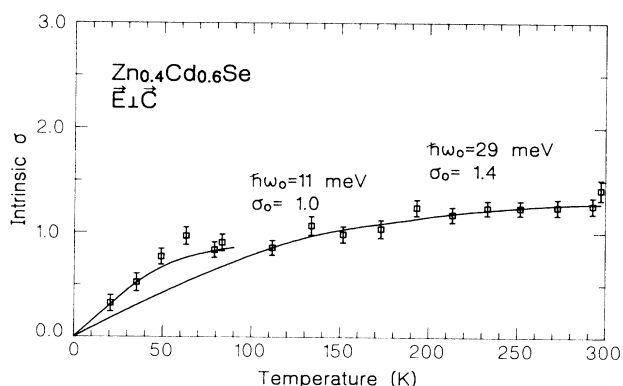


FIG. 5. Intrinsic σ vs temperature in $\text{Zn}_{0.4}\text{Cd}_{0.6}\text{Se}$, $\text{E} \perp \text{C}$ polarization.

TABLE I. The values of σ_0 and $\hbar\omega_0$ (of Urbach rule) in the two temperature ranges, and E_0 versus composition. H and C denote hexagonal and cubic, respectively.

X	Structure	Polarization	Low temperature		High temperature		E_0 (meV)
			$\hbar\omega_0$ (meV)	σ_0	$\hbar\omega_0$ (meV)	σ_0	
0	H	$E \perp c$	7.0	1.05	27.0	2.30	1.895
0.04	H	$E \perp c$	7.5	1.31	27.5	2.73	1.957
0.3	H	$E \parallel c$	9.0	1.05	28.5	2.70	2.182
0.3	H	$E \perp c$	9.0	0.61	28.5	2.31	2.148
0.4	H	$E \parallel c$	11.0	1.60	29.0	2.55	2.246
0.4	H	$E \perp c$	11.0	1.00	29.0	1.40	2.246
1	C		10.0	1.00	31.0	2.40	2.887

100 K the fields are induced by the piezoelectric LA phonons and at higher temperatures by LO phonons. The influence of the increasing disorder is observed in $\text{Zn}_{0.4}\text{Cd}_{0.6}\text{Se}$ by the greater divergence of the experimental results from the theoretical curve which corresponds to a well-ordered crystal. Further evidence for the increasing disorder is also observed in greater values of the σ parameter of the extrinsic absorption far below the absorption edge.

The continuous variation of the LO phonons energies with composition appears also in the value of the phonon energy $\hbar\omega_0$ on which the σ parameter depends. This variation of $\hbar\omega_0$ is in agreement with the results obtained by Raman spectra of such crystals. The value of E_0 also varies linearly with composition in the hexagonal crystals. The values of the σ_0 fitting parameter are similar in size to those of other pure II-VI compound single crystals.

APPENDIX

The theoretical basis for the DR theory is Elliott's²⁹ approach, which assumes the validity of the effective-mass approximation, and expresses the optical-absorption coefficient in terms of the wave function of the relative motion of the electron and the hole which constitute the exciton. Final-state^{17,30–34} interactions have to be introduced in order to obtain good agreement between the theory and experimental results. The resultant absorption

coefficient is

$$\alpha(E) \propto \epsilon_2(E) = C' \sum_{\mathbf{k}} |\langle U_{v-h}^e(\mathbf{r}) \rangle|^2 \times \delta(E - E_c(\mathbf{k}) + E_v(\mathbf{k})), \quad (\text{A1})$$

where $E = \hbar\omega$ is the photon energy, and C' is effectively constant over the relevant range of photon energies.

The application of a uniform electric field affects only the relative motions of the electrons and holes and not their free-particle-like center-of-mass motion, because the whole exciton is electrically neutral.

The relative motion wave function $U_v(\mathbf{r})$ solves the Schrödinger equation

$$\left[-\frac{\hbar^2}{2\mu} \nabla^2 - \frac{e^2}{\epsilon_0 r} - eF_e z \right] U_v(\mathbf{r}) = E_v U_v(\mathbf{r}), \quad (\text{A2})$$

where $r = |\mathbf{r}|$ is the exciton radius, and z is the direction of the applied field. The final-state interaction is represented by $e^2/2\epsilon_0 r$.

The absorption coefficient depends on the energy of the photon as

$$\alpha(E) \propto \sum_v |U_v(0)|^2 \delta(E - E_v), \quad (\text{A3})$$

where $|U_v(0)|^2$ is the electron-hole overlap squared, i.e., the probability that their spatial positions coincide.

In the absence of nonuniform electrostatic potentials in the crystal, the external electric field potential drop $-eF_e z$ is replaced by $V_e(\mathbf{R}_{cm}, \mathbf{r})$, which is the potential energy associated with the microfields in the crystal. (\mathbf{R}_{cm} is the position vector of the center of mass of the exciton.) The main possible sources for those microfields are charged impurities, disorder potential fluctuations, and LO phonons. In piezoelectric materials the microfields can be induced also by LA phonons.

One of the main features of this model is that it yields the exponential shape of the absorption coefficient independently of the microfields's sources and distribution.

The optical-absorption coefficient α , in the presence of a uniform electric field F has been shown to be field and energy dependent as

$$\alpha(E) \propto \exp \left[\frac{C}{F} (E - E_0) \right], \quad (\text{A4})$$

where C is a constant.

In the presence of various internal microfields (and ab-

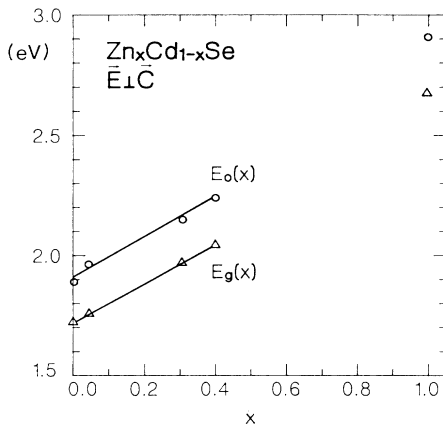


FIG. 7. Energy gap (measured at room temperature) and E_0 (of Urbach rule equation) vs composition.

sence of an external field), α is averaged over the whole field distribution $P(F)$

$$\langle \alpha(E) \rangle = \int P(F) \alpha(E, F) dF. \quad (\text{A5})$$

Since the field distribution $P(F)$ is sensitive to the source of the microfields, the thermal dependence of $\alpha(E)$ gives an indication as to this source.

Evaluation of $P(F)$, which begins with the Fröhlich Hamiltonian for the electron-phonon interaction, results after algebraic manipulations, in a Gaussian distribution of those fields

$$P(F) = \left[\frac{2\pi}{3} \langle F^2 \rangle \right]^{-3/2} 4\pi F^2 \exp \left[-\frac{3F^2}{2\langle F^2 \rangle} \right]. \quad (\text{A6})$$

Carrying out the integration $\int \alpha(E, F) P(F) dF$ yields

$$\langle F^2 \rangle = \frac{\hbar\omega_0}{3\pi\epsilon^*} q_c^3 \coth \left[\frac{\hbar\omega_0}{2kT} \right], \quad (\text{A7})$$

where q_c is the polaron cutoff, and $\epsilon^* = (1/\epsilon_\infty - 1/\epsilon_0)^{-1}$ is the effective dielectric constant.

The best evaluation for q_c , based on the uncertainty principle results in

$$(q_c a)^3 \simeq \frac{2\epsilon_0}{\pi E_b \epsilon^*} \hbar\omega_0 \coth \left[\frac{\hbar\omega_0}{2kT} \right], \quad (\text{A8})$$

where E_b is the binding energy of the 1S exciton, and a is its radius.

Taking E_b as equal to $e^2/2\epsilon_0 a$ yields

$$F_{\text{rms}} = \frac{2\epsilon_0}{\sqrt{3}\epsilon^* \pi e a} \coth \left[\frac{\hbar\omega_0}{2kT} \right]. \quad (\text{A9})$$

¹F. Urbach, Phys. Rev. **92**, 1324 (1953).

²W. Martienssen, J. Phys. Chem. Solids **2**, 257 (1957).

³G. Harbeke, in *Optical Properties of Solids*, edited by F. Abeles (North-Holland, Amsterdam, 1972), p. 33.

⁴J. Klafter and J. Jortner, Chem. Phys. **26**, 421 (1977).

⁵Ya. G. Klyava, Fiz. Tverd. Tela (Leningrad) **27**, 1350 (1985) [Sov. Phys.—Solid State **27**, 816 (1985)].

⁶M. V. Kurik, Phys. Status Solidi A **8**, 9 (1971).

⁷H. Miyazaki and E. Hanamura, J. Phys. Soc. Jpn. **50**, 1310 (1980).

⁸K. Kobayashi and T. Tomiki, J. Phys. Chem. Solids **22**, 73 (1961). For additional references for alkali halides, see Ref. 6.

⁹Y. Brada, B. G. Yacobi, and A. Peled, Solid State Commun. **17**, 193 (1975).

¹⁰M. Ya. Valakh *et al.*, Phys. Status Solidi B **113**, 635 (1982).

¹¹Yu. A. Mityagin *et al.*, Fiz. Tverd. Tela. **17**, 2054 (1975).

¹²D. Schmeltzer and R. Beserman, J. Phys. C **14**, 5003 (1981).

¹³R. Beserman and M. Balkanski, Phys. Rev. B **1**, 608 (1970).

¹⁴Y. Brada and L. Samuel, Phys. Rev. B **35**, 8260 (1987).

¹⁵Y. Toyozawa and M. Schreiber, J. Phys. Soc. Jpn. **51**, 1528 (1982).

¹⁶E. I. Rashba, in *Modern Problems in Condensed Matter Sciences*, edited by E. I. Rashba and M. D. Sturge (North-Holland, Amsterdam, 1982), Vol. 2, Chap. 13, p. 543.

¹⁷*Physics of II-VI and I-VII Compounds, Group III*, edited by O.

Madelung (Springer-Verlag, Berlin, 1982), Vol. 17.

¹⁸J. D. Dow and D. Redfield, Phys. Rev. B **5**, 594 (1972).

¹⁹J. D. Dow and D. Redfield, Phys. Rev. B **1**, 3358 (1970).

²⁰D. Redfield and M. A. Afromowitz, Appl. Phys. Lett. **11**, 138 (1967).

²¹J. Baillou *et al.*, J. Phys. Chem. Solids **41**, 295 (1980).

²²K. Cho, in *Topics in Current Physics*, edited by K. Cho (Springer, Berlin, 1979), Vol. 14, Chap. 5, p. 217.

²³J. D. Dow, M. Bowen, R. Bray, D. L. Spears, and K. Hess, Phys. Rev. B **10**, 4305 (1974).

²⁴A. Burger and M. Roth, J. Cryst. Growth **70**, 7 (1984).

²⁵L. Samuel, Y. Brada, A. Burger, and M. Roth, following paper, Phys. Rev. B **36**, 1174 (1987).

²⁶A. Balzarotti *et al.*, Phys. Rev. B **31**, 7526 (1985).

²⁷Y. Brada and A. Honig (unpublished).

²⁸J. D. Dow, D. L. Smith, and F. L. Lederman, Phys. Rev. B **8**, 4612 (1973).

²⁹R. J. Elliott, Phys. Rev. **108**, 1384 (1957).

³⁰D. F. Blossey, Phys. Rev. B **3**, 1382 (1971).

³¹J. D. Dow, B. Y. Lao, and S. A. Newman, Phys. Rev. B **3**, 2571 (1970).

³²J. D. Dow and D. Redfield, Phys. Rev. B **1**, 3358 (1969).

³³F. C. Weinstein, J. D. Dow, and B. Y. Lao, Phys. Rev. B **4**, 3502 (1971).

³⁴J. D. Dow, Surf. Sci. **37**, 786 (1973).